Research Article

Ioannis Moutzouris-Sidiris* and Konstantinos Topouzelis

Assessment of Chlorophyll-a concentration from Sentinel-3 satellite images at the Mediterranean Sea using CMEMS open source *in situ* data

https://doi.org/10.1515/geo-2020-0204
received June 01, 2020; accepted October 12, 2020

Abstract: The objective of this study is to evaluate the efficiency of two well-known algorithms (Ocean Colour 4 for MERIS [OC4Me] and neural net [NN]) used in the calculation of chlorophyll-a (Chl-a) from the Sentinel-3 Ocean and Land Colour Instrument (OLCI) compared to *in situ* measurements covering the Mediterranean Sea. *In situ* data set, obtained from the Copernicus Marine Environmental Monitoring Service (CMEMS) and more specifically from the data set with the title INSITU_MED_NRT_OBSERVATIONS_013_035, and Chl-a values at different depths were extracted. The concentration of Chl-a at a penetration depth was calculated. Then, water was classified into two categories, Case-1 and Case-2. For Case-2 waters, the OC4Me presents a moderate correlation with the *in situ* data for a time window of 0–2 h. In contrast with the NN algorithm, where very weak correlations were calculated, lower values of the statistical index of Bias for Case-1 waters were calculated for the OC4Me algorithm. Higher values of Pearson correlation were calculated ($r > 0.5$) for OC4Me algorithm than NN. OC4Me performed better than NN.

Keywords: Mediterranean Sea, remote sensing, Chlorophyll-a, Sentinel-3

*** Corresponding author: Ioannis Moutzouris-Sidiris,** Department of Marine Sciences, University of the Aegean, Mytilene, Greece, e-mail: moutzouris@aegean.gr, tel: +30-22-5103-6877
*** Corresponding author: Konstantinos Topouzelis,** Department of Marine Studies, University of Aegean, Mytilene, Greece, e-mail: topouzelis@marine.aegean.gr, tel: +30-22-5103-6878

1 Introduction

Chlorophyll-a (Chl-a) can absorb light, and it can use this energy as a fuel for photosynthesis. It can be considered as a proxy of the biomass of the phytoplankton species [1]. The concentration of Chl-a is considered to be a critical water quality parameter for many environmental issues such as eutrophication. Eutrophication can lead to severe outcomes for the aquatic environment, namely an increase in hypoxia, fish deaths and the presence of harmful algae [2,3].

Chl-a can be measured using various methods such as spectrophotometry, high-performance liquid chromatography (HPLC), and fluorometry. However, these methods require an experienced analyst to generate consistently efficient results. Moreover, for various reasons such as the need for collecting samples at regular time intervals, there is an inability to continuously monitor Chl-a [4]. Satellites can provide and improve the temporal and spatial distributions of Chl-a compared to *in situ* sampling. Satellite images could cover large water areas in terms of spatial and temporal requirements in contrast with field methods, where a lot of measurements would be needed.

Chl-a can be estimated by satellites using empirical, analytical, and semi-analytical methods. Empirical algorithms are calculated by statistical regression [5] or end-member selection [6]. Analytical algorithms are established by simplified solutions of the radiative transfer equation. Semi-analytical methods can be classified between the one's named analytical and the one's classified as empirical, and the techniques used are a combination of empirical and analytical. Other techniques include spectral inversion procedures, which match spectral measurements to bio-optical forward models [7].

Areas, which cannot be described by only one optical constituent of the water column, are named as Case-2 waters. Different substances, particulate compounds, a large variety of organic macromolecules, living organisms such as phytoplankton, zooplankton, bacteria, and

their debris, and excrements exist in the water column. All these have various optical properties in regard to scattering, absorption, and partly fluorescence [8]. In Case-2 waters, their optical properties are controlled not only by phytoplankton and other particles such as coloured dissolved organic matter but also by substances, such as inorganic particles in suspension and yellow substances. Models can also be applied in areas where the phytoplankton is the main component influencing the optical properties of the water column [9], known as Case-1 waters.

Various sensors have been used to estimate Chl-a, including Landsat, MERIS, MODIS [10], and hyperspectral systems [11]. Sensors such as MODIS, SeaWiFS, and MERIS have high temporal acquisition and bands ideally positioned for the detection of water quality parameters such as Chl-a. On the contrary, multispectral sensors such as Landsat, IKONOS, and SPOT have few broadbands with higher spatial resolutions (4–30 m) and are primarily designed for terrestrial applications [10].

In addition, several studies have been performed to calculate Chl-a in the Mediterranean Sea [12,13]. For example, in 2007, the SeaWiFS satellite was used for the calculation of Chl-a at the Mediterranean Sea, because standard algorithms named OC4v4, OC3, and Algal1 failed [12]. *In situ*, Chl-a and optical measurements were considered for the validation of two standard regional (named BRIC and DORMA) bio-optical algorithms and a global one (OC4v4). DORMA is based on an Ocean Colour 2 band algorithm (OC2). BRIC is a regional algorithm for the retrieval of Chl-a from SeaWiFS in oligotrophic conditions. The results of this study indicate that OC4v4 performed better than BRIC and DORMA. Furthermore, a new regional algorithm was developed, named Mediterranean Ocean-Colour 4 bands (MedOC4). The MedOC4 had the best performance because it minimized the difference between concentrations of Chl-a calculated from the satellite and the *in situ* measurements [12].

In 2012, a computing system consisting of three separate processing chains was developed for the calculation of water quality parameters such as Chl-a and attenuation coefficient by the Satellite Oceanography Group (GOS) of Rome [13]. It was designed for the study area of the Mediterranean and the Black Seas. This method was applied to the satellite data of SeaWiFS, MODIS-Aqua, and MERIS. Validation of the Chl-a derived from the satellite data with *in situ* measurements was performed. The *in situ* Chl-a data sets consisted of 21 cruises, covering different areas over the Mediterranean Sea and one fixed station located in Italy. SeaWiFS Chl-a product performed better over the Mediterranean Sea in comparison to those of MODIS and MERIS. Despite their good general agreement with *in situ* observations, MODIS and MERIS derived Chl-a showed an underestimation correlated with the *in situ* data [13]. In 2016, the Ocean and Land Colour Instrument (OLCI) was launched on board of Sentinel-3A, which was based on ENVISAT's Medium Resolution Imaging Spectrometer (MERIS). Compared to MERIS, a higher number of bands (21 instead of 15) and an improved temporal coverage of the global ocean (<4 days instead of approximately 15 days) were provided [14].

The main purpose of the present research is to evaluate the efficiency of algorithms used by Sentinel-3, for the calculation of Chl-a, with *in situ* data covering the Mediterranean Sea. An additional question of this paper, which was later considered, is to calculate the optimum time window for the best correlation between the Chl-a calculated from the satellite and the *in situ* data set. The time window is defined as the time difference between the *in situ* and the satellite measurements. The results are summarized in scatter plots and tables. Two algorithms were tested named Ocean Colour 4 for MERIS (OC4Me) and neural net (NN). OC4Me applies a fourth-order polynomial equation and a Maximum Band Ratio (MBR) between the irradiance reflectance at the wavelength of 443, 490, 510, and 555. NN uses an Inverse Radiative Transfer Model and neural networks to estimate the water constitutes.

2 Methods and materials

2.1 Study area

The study area is defined as the Mediterranean Sea, which is considered to be a mid-latitude, mostly oligotrophic and ultra-oligotrophic basin. Higher values of biomass and consequently of Chl-a may be found in areas influenced by river runoff or by deep convection events [15,16]. The Mediterranean Sea is regarded as a good oceanographic test area because of its complex ocean dynamics and its dense anthropogenic pressure [15]. A map that was created to illustrate the position of the *in situ* measurements and the area of study is shown in Figure 1. The *in situ* measurements used for the evaluation were selected based on the availability of satellite data at a similar date.

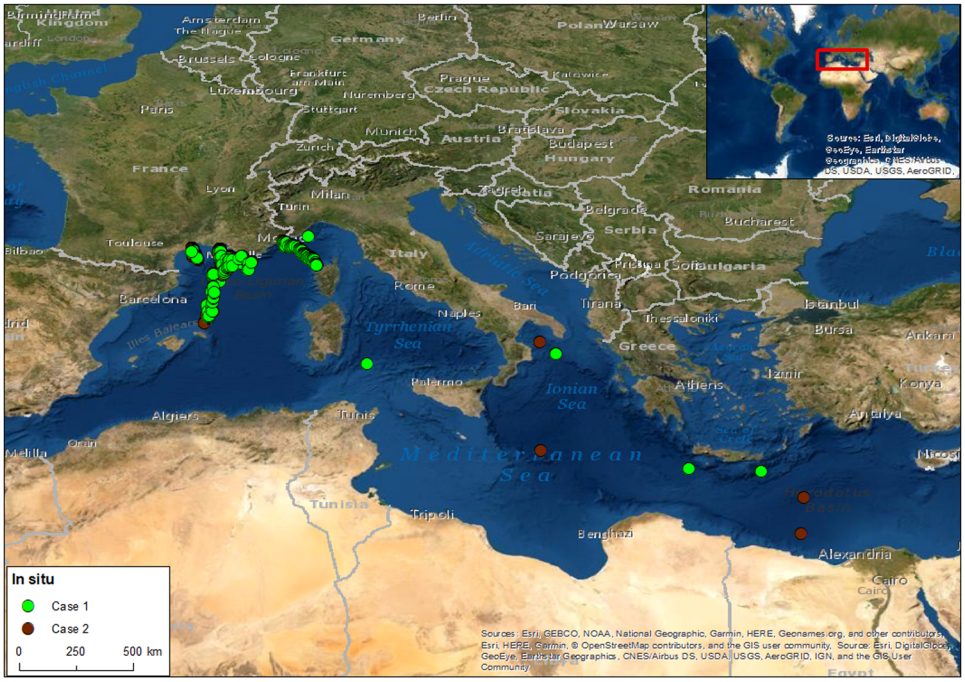

Figure 1: Area of study and points selected for the present study.

The points (*in situ* measurements) are spread in different areas across the Mediterranean Sea and more specifically at the Ionian Sea, Ligurian Sea, and the Tyrrhenian Sea. Nevertheless, the majority of them are concentrated in the Ligurian Sea.

An open-access data set from the Copernicus Marine Environmental Monitoring Service (CMEMS) with *in situ* Chl-a concentrations (INSITU_MED_NRT_OBSERVATIONS_013_035) was chosen for the comparison with the corresponding satellite data. Measurements of Chl-a fluorescence are saved in variable FLU2 [17]. The WGS84 geographic coordinate system was selected as the most appropriate one for the study. The applied *in situ* parameters from CMEMS representing Chl-a concentrations were Chl-a fluorescence (FLU2), Chl-a (CPHL), and Chl-a adjusted (CPHL_ADJUSTED). According to CMEMS, the CPHL_ADJUSTED refers to quality checked Chl-a and eventually corrected data. The measurements of Chl-a are always related to pressure or depth. A total of 67 NetCDF files with *in situ* measurements of Chl-a were initially downloaded. Files containing the variable CPHL were used for the comparison, because of the lack of satellite images for the rest of the *in situ* data set. Those NetCDF files contained a set of 692 points with *in situ* data which were selected for the comparison.

The Sentinel-3 satellite data considered in this study were acquired between the years 2016–2018. Sentinel-3 uses the OLCI instrument, which is an imaging spectrometer measuring solar radiation reflected by the earth. Compared to the MERIS satellite, it provides additional spectral channels, different camera arrangements, and simplified onboard processing. The Level 2 full resolutions (WFR) non-time critical (NTC) products of Sentinel-3 were selected, providing a good spatial resolution of 300 m and a temporal resolution of 1–3 days, depending on the region of interest. The satellite has 21 spectral bands ranging from 400 to 1020 nm [14]. The characteristics of the bands are presented in Table 1.

Two algorithms were examined on their efficiency on the estimation of the Chl-a from Sentinel-3 OLCI satellite data. These two algorithms are the OC4Me MBR and NN as referenced in ESA [14] and EUMETSAT [18]. Level 2 products of Sentinel-3 use the mentioned algorithms for the calculation of Chl-a. The algorithms are widely known and freely available to the public. Moreover, the focus of this study is not to calibrate or develop new algorithms rather than to test the ones used by Sentinel-3 OLCI satellite data.

A total of 114 images from Sentinel-3 were found to be appropriate for the comparison with the *in situ* data. The images were selected based on the sensing date which had to be the same as the date of the *in situ* measurement.

The methodology of our analysis was separated into two main parts. The first one consisted of processes for the *in situ* data and the second one of processes for the satellite data set. A flow diagram was prepared (Figure 2).

Table 1: Characteristics of the bands of Sentinel-3 OLCI [14]

Band	Central wavelength (nm)	Bandwidth (nm)
Oa1	400	15
Oa2	412.5	10
Oa3	442.5	10
Oa4	490	10
Oa5	510	10
Oa6	560	10
Oa7	620	10
Oa8	665	10
Oa9	673.75	7.5
Oa10	681.25	7.5
Oa11	708.75	10
Oa12	753.75	7.5
Oa13	761.25	2.5
Oa14	764.375	3.75
Oa15	767.5	2.5
Oa16	778.75	15
Oa17	865	20
Oa18	885	20
Oa19	900	10
Oa20	940	20
Oa21	1,020	40

2.1.1 Analysis of *in situ* measurements

Regarding the *in situ* measurements, the variables FLU2, CPHL, CPHL_ADJUSTED, LATITUDE, and LONGITUDE were extracted from the NetCDF (.nc) files downloaded from CMEMS. For the comparison with the satellite measurements, *in situ* data containing CPHL were used. To assure the quality of the *in situ* measurements, the quality controls provided by the CMEMS were taken into consideration. In Table 2, the values and the description of the quality controls are presented. Moreover, the POSITION_QC and the TIME_QC referring to quality controls for the time and position were used.

Data with quality controls 1, 2, and 7 were selected for the comparison with satellite data. In addition, negative *in situ* measurements of Chl-a were excluded. Chl-a values measured at different depth/pressure were preferred. The meaning of code 7 corresponds to measurements that could not be reported, e.g. a depth of a Chl-a concentration in this case the nominal values were used. Regarding the transformation of pressure to water depth, the methodology proposed by Saunders was applied [19]. It uses the following two equations that take into account the pressure in decibars (db) and the latitude:

$$c_1 = [5.92 + 5.25 \times \sin(\varphi \times 3.14/180)^2] \times 10^{-3}, \quad (1)$$

$$z = (1 - c_1) \times p - (2.21 \times 10^{-6}) \times (p^2), \quad (2)$$

where p is the water pressure in dbar, φ is the latitude in degrees, z is depth in metres, and c_1 is a function of latitude.

Verification of Chl-a calculated from the satellite data should be compared to the *in situ* concentration of Chl-a named C_M [15]. For the calculation of C_M, the following formula (equation 3) was applied [15].

$$C_M = \frac{\int_0^{z_{pd}} C(z) \times \exp\{-2 \times k_d \times z\} dz}{\int_0^{z_{pd}} \exp\{-2 \times k_d \times z\} dz}, \quad (3)$$

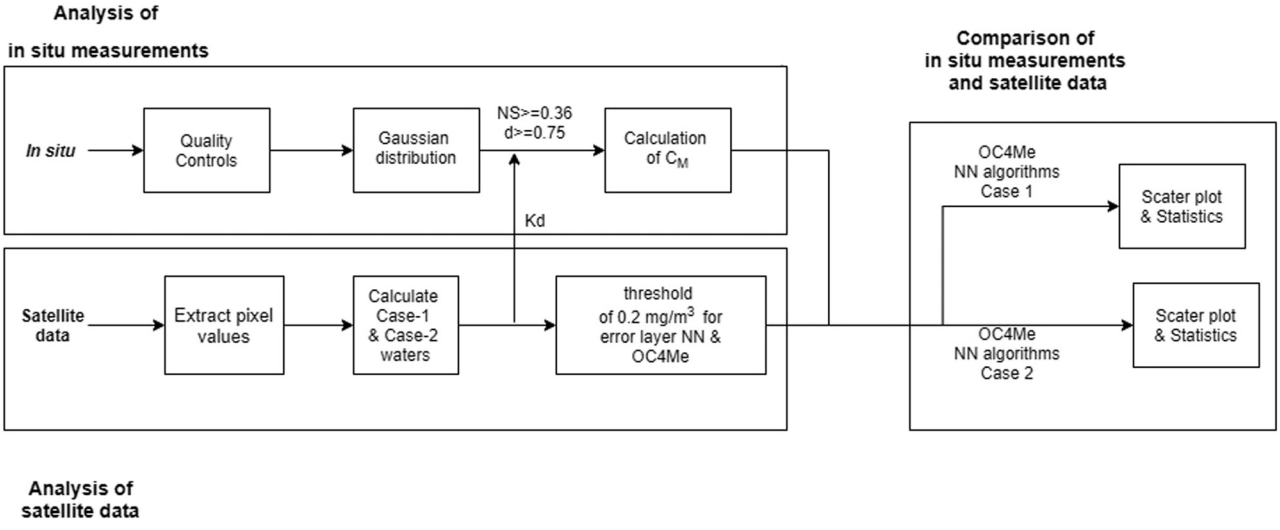

Figure 2: Flow diagram.

Table 2: Quality controls of *in situ* measurements [17]

Code	Meaning	Comment
0	No QC was performed	—
1	Good data	All real-time QC tests passed
2	Probably good data	—
3	Bad data that are potentially correctable	These data are not to be used without scientific correction
4	Bad data	Data have failed one or more of the tests
5	Value changed	Data may be recovered after transmission error
6	Not used	—
7	Nominal value	Data were observed but not reported. Example of an instrument target depth
8	Interpolated value	Missing data may be interpolated from neighbouring data in space or time
9	Missing value	An observation was performed, but is not available

where k_d is the attenuation coefficient, $C(z)$ is the measured Chl-a concentration expressed in mg m^{-3}, and Z_{pd} is called the penetration depth [20] and is defined as the inverse of the k_d (m^{-1}), and therefore, it can be calculated as $Z_{pd} = 1/k_d$ [21].

For the calculation of Chl-a (equation 3), the measured concentration should be calculated. It follows a Gaussian distribution [22]. Equation (4) is given by:

$$C(z) = B_0 + \frac{h}{\sigma\sqrt{2\times\pi}} \times e^{\frac{-(z-z_m)^2}{2\times\sigma^2}}. \quad (4)$$

The concentration of Chl-a at a specific depth ($C(z)$) depends on four parameters: the background Chl-a concentration (B_0), the height parameter (h), the width of the peak (σ), and the depth of the Chl-a peak (z_m). They were restrained to only positive values, because of the fact that negative numbers have no meaning [22]. A graph (Figure 3) is presented, showing a typical profile of Chl-a in relation to depth.

To specify the best fitting of the equation mentioned (equation 4), two statistical indexes (Nash–Sutcliffe coefficient [NS] and Willmott's index [d]) were determined. A good fit was considered when $d \geq 0.75$ and NS ≥ 0.36 [24]. For the parameters of the distributions to have a physical meaning, they were constrained to only positive values [23]. Regarding the satellite data, a matchup file was generated between the dates of the satellite data and the *in situ* measurements. For each *in situ* measurement, the corresponding pixel value was used. A window size with 1 × 1 pixel was taken into consideration for the matchup file and pixels identified as "water" were examined as well. The attenuation coefficient is a direct product of Sentinel-3 images and consequently, no estimation was needed. It was applied for the calculation of the Z_{pd}.

For the calculation of K_d, a semi-analytical approach is used from Sentinel-3 data, which is based in the addition of spectral inherent optical properties (IOPs), namely the absorption coefficient and the backscattering coefficient, into a solution of the radiative transfer equation. K_d is estimated for Case-1 waters. A linear relationship between K_d is established through statistical analyses of simultaneous field data from Chl-a. A more detailed description of the estimation of K_d can be found in Morel et al. [25].

2.1.2 Analysis of satellite data

Two algorithms were examined on their efficiency on the estimation of the Chl-a from satellite images: the OC4Me and a NN algorithm. In the first one, Chl-a is directly calculated using the MBR. The algorithm applies a fourth-order polynomial equation [18] and was developed by Morel et al. [25]. A more general description of

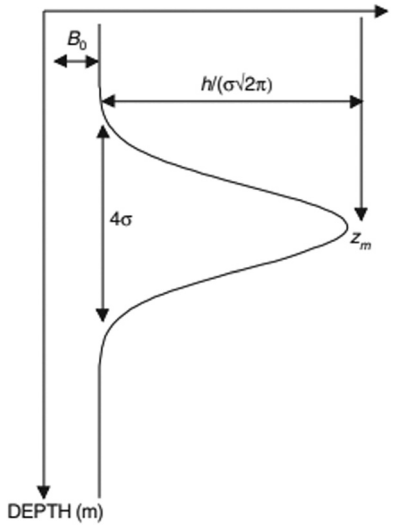

Figure 3: Typical profile of Chlorophyll-a with depth [23].

the algorithm can be found in the study of O'Reilly et al. [26].

$$C = 10^{A_0 + A_1 \times R + A_2 \times R^2 + A_3 \times R^3 + A_4 \times R^4}, \quad (5)$$

where R = log10 (MBR) and the coefficients $A_0 = 0.450$, $A_1 = -3.259$, $A_2 = 3.522$, $A_3 = -3.359$, and $A_4 = 0.949$; and C is the derived concentration of Chl-a in mg m^{-3}.

The MBR (equation 6) is calculated as follows:

$$\text{MBR} = \max((R_{443}, R_{490}, R_{510})/R_{555}), \quad (6)$$

where R_{443}, R_{490}, R_{510}, and R_{555} are the irradiance reflectance at the wavelength of 443, 490, 510, and 555 nm, respectively, as it is described by EUMETSAT [18]. Relevant nominal band used by Sentinel-3 OLCI at the wavelength of 555 is 560 nm.

The second algorithm, i.e. NN, uses an Inverse Radiative Transfer Model to estimate the water constitutes. It was initially developed by Doerffer and Schiller for Case-2 waters [8]. Later, it was updated to become the Case-2 Regional/Coast Colour (C2RCC) processor applied by Sentinel-3. The processor relies on an extensive database of simulated water leaving reflectance and related top-of-atmosphere radiances. Neural networks are trained in the inversion of the spectrum for atmospheric correction, as well as the retrieval of IOPs of the water body. The IOPs were then converted into Chl-a and a total suspended matter concentration using arithmetic conversion factors.

The methodology proposed by Matsushita et al. was selected for distinguishing Case-1 from Case-2 waters [27]. Case-1 waters should satisfy the following relationship (equation 7):

$$\alpha_{412}/\alpha_{443} \leq 1.2, \quad (7)$$

where α is defined as the absorption coefficient at 412 and 443 nm wavelengths.

The last equation can be related to the reflectance ratio between the values at 412 and 443 nm having a number greater than one or equal to one as described by Matsushita et al. [27]. Thus, a comparison of the reflectance calculated at the wavelengths of 412 and 443 nm is applied. If the reflectance at 412 nm is higher than or equal to the one at 443 nm, then the pixel is Case-1 water. Otherwise, it must be considered as Case-2 water. Moreover, the two algorithms had relevant error layers. A threshold of 0.2 mg m^{-3} to the error layers was applied for both cases to avoid measurements with severe errors. In the study of Bulgarelli and Zibordi, the same can be seen with respect to reflectance at 412 nm having lower values than at 443 nm for Case-2 waters [28].

In regard to the Sentinel-3 images, they were selected based on the sensing date which had to be the same as the date of the *in situ* measurement. Images, where Gaussian distributions could not be fitted with the *in situ* data (which will be described in Section 1.1), were excluded.

Moreover, the Chl-a calculated from the satellite, using the two algorithms (OC4Me and NN), is always estimated for the euphotic zone.

2.1.3 Comparison of *in situ* measurements and satellite data

Generally, the time window in the bibliography varies from 8 to 12 h [15]. The described process was performed for different ranges of time windows (0–7 h) for Case-1 and Case-2 waters accordingly. Therefore, another question was raised, regarding the optimum time window for the best correlation between the Chl-a calculated from the satellite and the *in situ* data set.

To validate Chl-a calculated from satellite data against the corresponding *in situ* values, statistical indexes (coefficients of determination [r^2], Pearson correlations [r], and Bias) were calculated. The indexes that were applied are the following ones (Table 3).

To test the level of significance of a correlation coefficient, a t-test was performed. The equation used to calculate the t-statistic is the following:

$$t = \frac{r \times (\sqrt{n-2})}{1 - r^2},$$

where n is the number of measurements, r is the Pearson correlation, and r^2 is the coefficient of determination.

Then a p-value using a Student T distribution output was generated (TDIST function in Microsoft excel). A two-tailed distribution and a significance level of 0.05 (α = 0.05) were selected. It was compared with a significance level of 0.05. If the p-value is less than the significance

Table 3: Statistical indexes

Statistical index	Equation	Units
r^2	$r^2 = \left(\frac{\sum_{i=1}^{N}[(y_i - \bar{y}) \times (x_i - \bar{x})]}{\sqrt{\sum_{i-1}^{N}[(y_i - \bar{y})]^2 \sum_{i=1}^{N}[(x_i - \bar{x})]^2}} \right)^2$	—
r	$r = \frac{\sum_{i=1}^{N}[(y_i - \bar{y}) \times (x_i - \bar{x})]}{\sqrt{\sum_{i-1}^{N}[(y_i - \bar{y})]^2 \sum_{i=1}^{N}[(x_i - \bar{x})]^2}}$	—
Bias	$\text{bias} = \frac{1}{N} \times \sum_{i=1}^{N}(y_i - x_i)$	mg m^{-3}

y is the value of Chl-a calculated from the satellite data and $\bar{y}$ is the mean value of y. x is the *in situ* value of Chl-a and $\bar{x}$ is the mean value of x. N is the number of measurements.

level, there is a significant linear relationship between the Chl-a calculated from the *in situ* and the satellite data.

Because of the large amount of data, code in the programming language of Python was written for several steps of the proposed methodology such as extracting parameters of interest from the NetCDF files, fitting Gaussian distributions as described in equation (4), getting pixel information in the selected longitudes and latitudes from the images, and finally for the validation of the results. Moreover, a geodatabase was constructed with tables and queries for the processing and organization of the data. In addition, Modelbuilder in ArcGIS was applied to make spatial joins for the *in situ* and the relevant images.

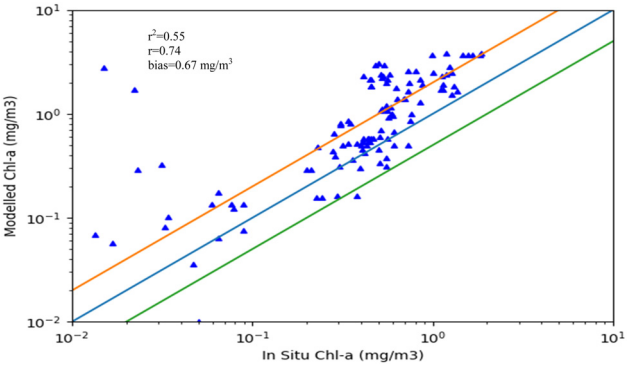

Figure 4: Scatter plot of *in situ* and modelled Chl-a using OC4Me algorithm for Case-2 waters with time window 0–2 h (1:1 line [blue line], 2:1 [orange line], and 1:2 [green line]; r^2 coefficient of determination, r Pearson correlation, bias).

3 Results

Two data sets were created, one with *in situ* measurements from CMEMS and one with Sentinel-3 satellite data. To eliminate possibly incorrect measurements, quality controls provided by CMEMS were applied. The *in situ* data set included values ranging from 0.01 to 4 mg m^{-3}, which were compared to Chl-a calculated from the satellite data. Two algorithms (OC4Me and NN) used by the Sentinel-3 satellite were evaluated. Case-1 and Case-2 waters were distinguished, based on the reflectance on the wavelengths of 412 and 443 nm.

The performance of the OC4Me algorithm with the *in situ* data set for the calculation of Chl-a was examined. Figure 4 and Table 4 illustrate the results. Figure 4 shows the *in situ* and the modelled concentrations plotted in a scatter plot for a time window of 0–2 h for Case-2 waters. The rest of the scatter plots for Case-1 and Case-2 are shown in Appendix (Figures A1a–g and A2a–g). In similar studies, a logarithmic scale was used in the scatter plots. An additional reason for using a log scale is to clearly visualize Chl-a concentrations, derived from *in situ* and satellite data. Table 4 illustrates basic statistical values calculated for the *in situ* and the modelled Chl-a of Case-1 and Case-2 waters using OC4Me algorithm.

In Figure 4, the modelled concentrations of Chl-a did not exceed 4 mg m^{-3}. *In situ* concentrations starting from 0.01 to more than 1 mg m^{-3} were estimated. Very few measurements exceed the green line having slopes less than 0.5. The rest of the measurements are spread between slopes greater than 1/2 (green line) and 0.5. Moreover, an overestimation of the modelled Chl-a can be observed.

In Table 4, the minimum values of the modelled and *in situ* data sets are similar for both Case-1 and Case-2 waters ranging from 0.01 to 0.08 mg m^{-3}. Similar mean values are observed for the *in situ* values regardless of the time window for Case-1 and Case-2 waters ranging from 0.47 to 0.78 mg m^{-3}. For the modelled concentrations, the values of the statistics (mean, max) for Case-1 are closer to the corresponding *in situ* measurements. The maximum (max) values of the modelled concentrations calculated for Case-1 are lower than the ones of Case-2. As the time difference increases, the concentrations observed (Case-1 and Case-2) are higher for most of the statistical values. Furthermore, an overestimation is observed (mean values) concerning the Case-2 waters, whereas in Case-1 waters, the *in situ* and the modelled mean values are very close.

Using the data sets created for the different ranges of time windows, the coefficient of determination, Pearson correlation, p-values, Bias, and the number of points were calculated, and they are presented in Table 5.

For Case-1 and Case-2, the best coefficient is calculated for a time window from 0 to 2 h having a value of 0.39 and 0.55, respectively. For Case-1, the coefficient of determination ranges from 0.25 to 0.39, and for Case-2 from 0.31 to 0.55. It is noteworthy that as the time window increases, the coefficient increases for Case-1 but decreases for Case-2. Correlation can be described by Evans [29].

Therefore, for Case-2 the correlation for the time windows of 0–2 h and 0–1 h can be considered as "moderate." For time windows greater than 2 h, correlations can be considered as "weak." For Case-1, they can be characterized as "weak." Pearson correlations were calculated for Case-1 and Case-2 waters with values higher

Table 4: Basic statistical properties of Case-1 and Case-2 waters using OC4Me algorithm

Time window (h)	*In situ* concentrations (mg m^{-3})						Modelled concentrations (mg m^{-3})					
	Case-1			Case-2			Case-1			Case-2		
	Min.	Max.	Mean	Min.	Max.	Mean	Min.	Max.	Mean	Min.	Max.	Mean
0–1	0.02	1.61	0.49	0.02	1.83	0.53	0.08	2.66	0.54	0.01	3.83	1.21
0–2	0.02	1.61	0.47	0.01	1.86	0.56	0.04	2.66	0.46	0.01	3.83	1.23
0–3	0.02	1.61	0.49	0.01	2.10	0.61	0.04	2.66	0.46	0.01	3.97	1.19
0–4	0.01	2.03	0.55	0.01	2.57	0.66	0.01	2.76	0.51	0.01	3.97	1.21
0–5	0.01	3.06	0.61	0.01	2.57	0.70	0.01	2.76	0.52	0.01	3.97	1.23
0–6	0.01	3.06	0.63	0.01	3.56	0.72	0.01	2.76	0.5	0.01	3.97	1.20
0–7	0.01	3.65	0.66	0.01	3.89	0.78	0.01	2.76	0.5	0.01	3.97	1.21

than 0.5 ($r \geq 0.5$) indicating a strong correlation between Chl-a calculated from the satellite and the *in situ*. All the p-values estimated for the different time windows and Cases are lower than 0.05; therefore, the relationship between calculated Chl-a from the satellite and the *in situ* data set is statistically significant.

In comparison to the r^2, the statistical index of the Bias gets its higher values for Case-2. Having a negative or a positive value can show an overestimation or an underestimation of the Chl-a calculated from the satellite. It varies from –0.16 to 0.05 mg m^{-3} (Case-1) and from 0.43 to 0.68 mg m^{-3} (Case-2). Moreover, the number of points can play an essential role in the values calculated from the statistical index of Bias. The number of points selected for the validation of Case-2 is higher than the corresponding value of Case-1. In general, the OC4Me algorithm performs better for Case-2 waters in terms of the coefficient of determination having higher coefficients. However, in terms of the statistical index of Bias, OC4Me algorithm performs better for Case-1 waters.

The efficiency of the NN algorithm for the calculation of Chl-a was examined as well (Figure 5 and Table 6). Figure 5 shows the *in situ* and the modelled concentrations plotted in a scatter plot for a time window of 0–2 h for Case-2 waters. The rest of the scatter plots for Case-1 and Case-2 are shown in Appendix (Figures A3a–g and A4a–g). Table 6 shows some basic statistical values for the *in situ* and the modelled Chl-a based on the distinction of Case-1 and Case-2 waters.

In Figure 5, it is observed that the modelled concentrations of Chl-a did not exceed 1 mg m^{-3}. *In situ* concentrations starting from 0.01 to more than 1 mg m^{-3} were estimated. A higher number of values exceed the green line having slopes less than 0.5 in the case of NN algorithm in comparison to the OC4Me, where very few data were estimated (Figure 4). In addition, an underestimation of the modelled Chl-a can be observed.

In Table 6, the minimum values of the modelled and *in situ* data sets are similar for both Case-1 and Case-2 waters ranging from 0.01 to 0.05 mg m^{-3}. Similar mean values are observed for the *in situ* values regardless of the time window for Case-1 and Case-2 waters ranging from 0.44 to 0.76 mg m^{-3}. Not very high differences in the modelled concentrations are observed between Case-1 and Case-2. As the time difference increases, the concentrations observed (Case-1 and Case-2) are higher in most of the statistics.

Using the data sets created for the different ranges of time windows, the coefficient of determination, Pearson correlation, p-values, Bias, and number of points were calculated and are presented in Table 7.

For Case-1 and Case-2, the best coefficient is calculated for a time window from 0 to 2 h having a value of 0.09 and 0.16 accordingly. The statistical index of Bias is always negative, indicating an underestimation of Chl-a from the satellite data. It ranges from –0.15 to –0.45 mg m^{-3} for Case-2 and from –0.23 to –0.40 mg m^{-3} for Case-1. As the time window increases, a higher underestimation is introduced to our data sets. Following the classification described by Evans [29], all the correlations can be characterized as "very weak". The number of points considered for the validation of Case-2 is higher than of Case-1.

For Case-1, Case-2, and time window 0–1 h, no correlation was estimated ($r < 0.3$) using Pearson correlation. For the rest of time windows and Case-1 waters, values higher than 0.3 and lower than 0.5 ($0.3 \leq r \leq 0.5$) indicate a moderate strength of correlation. For Case-2 and time windows 0–3 and 0–4, a weak strength of correlation was estimated. For the rest of Case-2 and time windows, a moderate strength of correlation was calculated. All the p-values estimated for the different time windows and Cases are lower than 0.05 therefore, the relationship between calculated Chl-a from the satellite and the *in situ* data set is statistically significant.

Table 5: Statistical indexes of Case-1 and Case-2 waters using OC4Me algorithm

Time window (h)	Case-1					Case-2				
	r^2	r	p-value	Bias (mg m^{-3})	Number of points	r^2	r	p-value	Bias (mg m^{-3})	Number of points
0–1	0.25	0.50	3.0×10^{-3}	0.05	33	0.51	0.71	1.2×10^{-8}	0.68	48
0–2	0.39	0.62	2.8×10^{-9}	−0.01	74	0.55	0.74	3.8×10^{-21}	0.67	114
0–3	0.39	0.62	1.8×10^{-12}	−0.03	103	0.37	0.61	2.1×10^{-19}	0.58	178
0–4	0.31	0.56	1.7×10^{-13}	−0.04	149	0.32	0.57	8.7×10^{-22}	0.55	241
0–5	0.37	0.61	6.5×10^{-21}	−0.09	193	0.31	0.56	3.0×10^{-25}	0.53	293
0–6	0.37	0.61	5.9×10^{-24}	−0.12	223	0.33	0.57	4.0×10^{-32}	0.49	350
0–7	0.35	0.59	1.7×10^{-26}	−0.16	266	0.34	0.58	1.0×10^{-39}	0.43	421

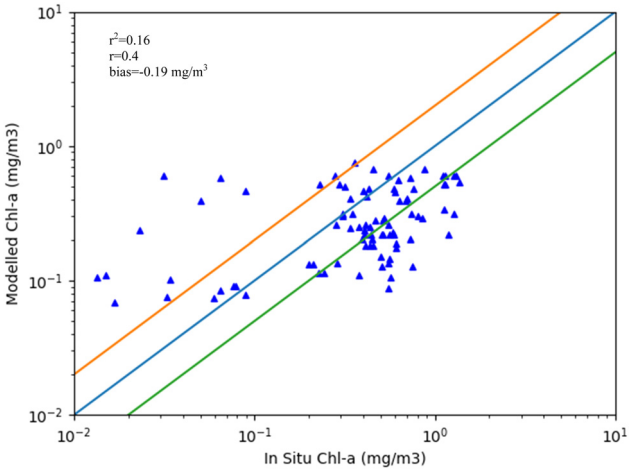

Figure 5: Scatter plot of *in situ* and modelled Chl-a using NN algorithm for Case-2 waters with time window 0–2 h (1:1 line [blue line], 2:1 [orange line], and 1:2 [green line]; r^2 coefficient of determination, r Pearson correlation, bias).

4 Discussion

By comparing Tables 5 and 7, "very weak" correlations are estimated using the NN algorithm in comparison with OC4Me, where "weak" to "moderate" correlations were calculated. Moreover, higher values of the statistical index Bias for Case-1 waters were calculated for the NN (−0.23 to −0.40 mg m^{-3}) algorithm compared to OC4Me (−0.16 to 0.05 mg m^{-3}). Higher values of Pearson correlations were estimated ($r > 0.5$) for OC4Me algorithm than NN. For Case-2 and time windows 0–1 h, 0–2 h greater values were calculated for r and strong correlations could be observed. Thus, OC4Me performed better than the NN algorithm having higher r^2 and r for both Case-1 and Case-2 waters and lower values of Bias for Case-1. The optimum time window was estimated at around 0–2 h using OC4Me, having the best coefficient of determination and a strong correlation between Chl-a calculated from the satellite and the *in situ* data set.

The variant number of points selected for the validation in all cases can influence the results of the statistical index of Bias, r^2. Generally, the values calculated for the coefficient of determination, using OC4Me and NN algorithm accordingly, cannot be considered sufficient for any remote-sensing product that could be applied in quantitative observation of phytoplankton biomass.

The NN algorithm of Sentinel-3 was designed for Case-2 waters. The Chl-a calculated from NNs requires a careful and elaborate determination of the multiple coefficients (training phase) [30]. Using a training data set may improve the calculation of Chl-a [31]. Consequently,

Table 6: Basic statistical properties of Case-1 and Case-2 waters using NN algorithm

Time window (h)	*In situ* concentrations (mg m^{-3})						Modelled concentrations (mg m^{-3})					
	Case-1			Case-2			Case-1			Case-2		
	Min.	Max.	Mean	Min.	Max.	Mean	Min.	Max.	Mean	Min.	Max.	Mean
0–1	0.02	1.22	0.44	0.03	1.19	0.49	0.05	0.70	0.21	0.07	0.75	0.34
0–2	0.02	1.27	0.44	0.01	1.37	0.49	0.03	0.72	0.22	0.07	0.75	0.31
0–3	0.02	1.54	0.47	0.01	2.10	0.55	0.03	1.20	0.22	0.07	0.78	0.29
0–4	0.02	2.03	0.52	0.01	2.57	0.62	0.03	1.20	0.22	0.06	0.93	0.29
0–5	0.01	2.31	0.58	0.01	2.57	0.67	0.02	1.20	0.21	0.06	1.20	0.29
0–6	0.01	2.31	0.60	0.01	3.56	0.68	0.02	1.20	0.21	0.06	1.20	0.30
0–7	0.01	2.31	0.61	0.01	3.89	0.76	0.02	1.20	0.21	0.06	1.20	0.31

the lack of them could explain the behaviour of the algorithm with the *in situ* concentrations.

One of the validations of this algorithm was performed using the Mermaid (status of 2012) *in situ* data set. A mean Bias of –0.21 mg m^{-3} was calculated for cases with high sun glint and an additional one of –0.27 mg m^{-3} without high sun glint. The coefficients applied in the equation for the calculation of Chl-a were obtained from data of the North Sea by regression [32]. Similar values with the ones calculated in regard to the statistical index of Bias can also be found to the study previously mentioned.

In Tilstone et al. [33], measurements from stations across the North Sea, English Channel, Celtic Sea, Mediterranean Sea, and along the Iberian coast were considered between June 2001 and March 2012. The accuracy of a range of ocean colour Chl-a was assessed, using two different atmospheric corrections (AC) processors (COASTCOLOUR and MERIS Ground Segment processor version 8.0 – MEGS8.0), in the North-West European waters. For the calculation of Chl-a, various algorithms such as the OC4Me were applied. Using the two mentioned processors (COASTCOLOUR and MEGS8.0) and the OC4Me algorithm for the estimation of Chl-a, coefficients of determinations were calculated with a value of 0.67 and 0.55 accordingly. In the present study, the best value was estimated using the OC4Me algorithm for Case-2 with 0.55, which is close to the study mentioned above. Furthermore, in the paper of Tilstone et al. [33], a NN algorithm similar to the one considered here was applied. A coefficient of 0.61 and 0.31 using the COASTCOLOUR and the MEGS8.0 AC models was estimated accordingly. Therefore, the AC method may play a significant role in the results [33].

Another study performed by Toming et al. [34] at the Baltic Sea calculated similar results regarding the coefficient of determination. It reported an r^2 up to 0.56 in coastal waters (R/V Salme measurements) and 0.43 in the open parts of the Baltic Sea (FerryScope measurements).

The attenuation coefficient at 490 nm was taken into account for the calculation of Chl-a at the penetration depth from the *in situ* data. This is a direct product of Sentinel-3. It was designed for Case-1 waters [25]. Considering an attenuation coefficient for Case-2, thus calculating the concentration of Chl-a at the penetration depth more accurately, may improve the results of the statistical indexes calculated for them.

For both cases, another significant uncertainty is the accuracy of the *in situ* data set. The only way to check the accuracy of the *in situ* data set considered is through the quality controls provided by the CMEMS. The quality controls do not produce a number specifying the accuracy but offer only descriptive information, which may be not sufficient. Other issues with the *in situ* could arise from various sources.

The unawareness of the exact kinds of methods, which were applied to produce the *in situ* data such as spectrophotometry or HPLC, may cause different uncertainties in our results. For example, not knowing the methodologies to derive the *in situ* Chl-a from CMEMS may influence the performance of the algorithms. In the work of Santos Dos et al. [35] different types of field methods were used to estimate Chl-a. Two of them, spectrophotometric and fluorimetric, had overestimated the Chl-a concentration.

As mentioned in CMEMS, the *in situ* data set is estimated from several methods from various institutions and researchers. If Chl-a values were derived from fluorescence data, then *in situ* concentrations could be a poor proxy to compare it with Chl-a calculated from satellite data.

Table 7: Statistical indexes of Case-1 and Case-2 waters using NN algorithm

Time window (h)	Case-1					Case-2				
	r^2	r	p-value	Bias (mg m^{-3})	Number of points	r^2	r	p-value	Bias (mg m^{-3})	Number of points
0–1	0.0001	0.01	9.58×10^{-1}	−0.23	30	0.03	0.17	3.12×10^{-1}	−0.15	36
0–2	0.09	0.30	1.36×10^{-2}	−0.23	67	0.16	0.40	1.03×10^{-4}	−0.19	89
0–3	0.15	0.39	1.25×10^{-4}	−0.25	93	0.07	0.26	1.58×10^{-3}	−0.27	140
0–4	0.12	0.35	5.79×10^{-5}	−0.3	129	0.07	0.26	1.86×10^{-4}	−0.33	195
0–5	0.14	0.37	7.39×10^{-7}	−0.36	165	0.1	0.32	7.44×10^{-7}	−0.37	235
0–6	0.14	0.37	8.98×10^{-8}	−0.39	192	0.15	0.39	1.14×10^{-11}	−0.38	286
0–7	0.12	0.35	7.41×10^{-8}	−0.4	229	0.16	0.40	1.31×10^{-14}	−0.45	343

Variabilities in the sample collection strategies (i.e. sampler type, depth(s), etc.) may produce differences in the measured *in situ* Chl-a values. *In situ* being collected at different periods under various potential circumstances, waters with low or high turbidity, and at different weather conditions could affect the accuracy of the measurements. Thus, all the mentioned uncertainties could affect the quality of the *in situ* data set and explain the performances of the algorithms.

Initially, the *in situ* data set was planned to be distinguished between coastal and oceanic stations; however, the *in situ* metadata from the CMEMS did not allow such discrimination.

5 Conclusions

In this study, the efficiency of two algorithms, the OC4Me MBR based on a polynomial algorithm and the NN Chl-a concentration based on an Inverse Radiative Transfer Model, was tested against open access *in situ* measurements. The *in situ* data set obtained from the CMEMS with Chl-a concentrations (INSITU_MED_NRT_OBSERVATIONS_013_035) was elected for the comparison with the Sentinel-3 satellite data.

We conclude in "very weak" correlations between the Chl-a calculated from the NNs and the corresponding *in situ* data. On the contrary, the OC4Me model of the ocean colour had a better performance with the *in situ* data set classified from "weak" to "moderate." Lower values of the statistical index of Bias for Case-1 waters were calculated for the OC4Me algorithm. Higher values of Pearson correlation were estimated ($r > 0.5$) for OC4Me algorithm than NN. For Case-2 and time windows 0–2, greater values for r were calculated and strong correlations could be observed. Therefore, OC4Me performed better than NN. The optimum time window was estimated at around 0–2 h, having a high coefficient of determination and a Pearson correlation. Concentrations higher than 4 mg m^{-3} were not tested. Generally, not sufficient correlations could be calculated between the *in situ* and the satellite data because of potential uncertainties arising from the quality of the *in situ* data.

Acknowledgements: This research has been co-financed by the European Regional Development Fund of the European Union and Greek national funds through the Operational Program Competitiveness, Entrepreneurship, and Innovation, under the call RESEARCH–CREATE–INNOVATE (project code: T1EDK-02966).

References

[1] Watanabe FSY, Alcântara E, Stech JL. High performance of chlorophyll-a prediction algorithms based on simulated OLCI Sentinel-3A bands in cyanobacteria-dominated inland waters. Adv Space Res. 2018;62:265–73.

[2] Ferreira JG, Andersen JH, Borja A, Bricker SB, Camp J, Cardoso da Silva M, et al. Overview of eutrophication indicators to assess environmental status within the European marine strategy framework directive. Estuarine Coastal Shelf Sci. 2011;93:117–31.

[3] Boesch DF. Challenges and opportunities for science in reducing nutrient over-enrichment of coastal ecosystems. Estuaries. 2002;25:886–900.

[4] Environmental YSI. The basics of chlorophyll measurement; 2013. p. 1–3

[5] Kabbara N, Benkhelil J, Awad M, Barale V. Monitoring water quality in the coastal area of Tripoli (Lebanon) using high-resolution satellite data. ISPRS J Photogramm Remote Sens. 2008;63:488–95.

[6] Tyler AN, Svab E, Preston T, Présing M, Kovács WA. Remote sensing of the water quality of shallow lakes: a mixture modelling approach to quantifying phytoplankton in water characterized by high-suspended sediment. Int J Remote Sens. 2006;27:1521–37.

[7] Odermatt D, Gitelson A, Brando VE, Schaepman M. Review of constituent retrieval in optically deep and complex waters from satellite imagery. Remote Sens Environ. 2012;118:116–26.

[8] Doerffer R, Schiller H. The MERIS Case 2 water algorithm. Int J Remote Sens. 2007;28:517–35.

[9] Antoine D. Sentinel-3 optical products and algorithm definition. OLCI level 2 algorithm theoretical basis document. ocean color products in case 1 waters; 2010. p. 1–19.

[10] Matthews MW. A current review of empirical procedures of remote sensing in Inland and near-coastal transitional waters. Int J Remote Sens. 2011;32:6855–99.

[11] Olmanson LG, Brezonik PL, Bauer ME. Airborne hyperspectral remote sensing to assess spatial distribution of water quality characteristics in large rivers: the Mississippi River and its tributaries in Minnesota. Remote Sens Environ. 2013;130:254–65.

[12] Volpe G, Santoleri R, Vellucci V, Ribera d'Alcalà M, Marullo S, D'Ortenzio F. The colour of the Mediterranean Sea: global versus regional bio-optical algorithms evaluation and implication for satellite chlorophyll estimates. Remote Sens Environ. 2007;107:625–38.

[13] Volpe G, Colella S, Forneris V, Tronconi C, Santoleri R. The Mediterranean ocean colour observing system-system development and product validation. Ocean Sci. 2012;8:869–83.

[14] ESA. Sentinel-3 user handbook; 2013.

[15] D'Ortenzio F, Marullo S, Ragni M, D'Alcalà MR, Santoleri R. Validation of empirical SeaWiFS algorithms for chlorophyll-a retrieval in the Mediterranean Sea: a case study for oligotrophic seas. Remote Sens Environ. 2002;82:79–94.

[16] Antoine D, Morel A, Andre JM. Algal pigment distribution and primary production in the eastern Mediterranean as derived from coastal zone color scanner observations. J Geophys Res. 1995;100:16193–209.

[17] Jaccard P, Hjemann DO, Ruohola J, Marty S, Kristiansen T, Sorensen K, et al. Copernicus marine environment monitoring service. Quality control of biogeochemical measurements; 2018.

[18] Eumetsat. Sentinel-3 OLCI marine user handbook; 2018.

[19] Saunders MP. Practical conversion of pressure to depth. Phys Oceanogr. 1981;11:573–4.

[20] Clark DK. Bio-optical algorithms – Case 1 waters (ATBD 17, v1.2). Ocean color web page; 1997. p. 1–52.

[21] Strass VH. Meridional and seasonal variations in the satellite-sensed fraction of euphotic zone chlorophyll. J Geophys Res. 1990;95:18289–301.

[22] Platt T, Caverhill C, Sathyendranath S. Basin-scale estimates of oceanic primary production by remote sensing: the North Atlantic. J Geophys Res. 1991;96:15147.

[23] Silulwane NF, Richardson AJ, Shillington FA, Mitchell-Innes BA. Identification and classification of vertical chlorophyll patterns in the Benguela upwelling system and Angola-Benguela front using an artificial neural network. South Afr J Mar Sci. 2001;23:37–51.

[24] Lopes FB, Novo EMLdM, Barbosa CCF, Andrade EMd, Ferreira RD. Simulation of spectral bands of the MERIS sensor to estimate chlorophyll-a concentrations in a reservoir of the semi-arid region. Rev Agro@mbiente On-line. 2016;10:96.

[25] Morel A, Huot Y, Gentili B, Werdell PJ, Hooker SB, Franz BA. Examining the consistency of products derived from various ocean color sensors in open ocean (Case 1) waters in the perspective of a multi-sensor approach. Remote Sens Environ. 2007;111:69–88.

[26] O'Reilly JE, Maritorena S, Mitchell BG, Siegel DA, Carder KL, Garver SA, et al. Ocean color chlorophyll algorithms for SeaWiFS. J Geophys Research: Ocean. 1998;103:24937–53.

[27] Matsushita B, Yang W, Chang P, Yang F, Fukushima T. A simple method for distinguishing global Case-1 and Case-2 waters using SeaWiFS measurements. ISPRS J Photogramm Remote Sens. 2012;69:74–87.

[28] Bulgarelli B, Zibordi G. On the detectability of adjacency effects in ocean color remote sensing of mid-latitude coastal environments by SeaWiFS, MODIS-A, MERIS, OLCI, OLI and MSI. Remote Sens Environ. 2018;209:423–38.

[29] Evans JD. Straightforward statistics for the behavioral sciences. Pacific Grove: Brooks/Cole Pub. Co.; 1996.

[30] IMT Neural Net; 2019. Available from: https://sentinels.copernicus.eu/web/sentinel/technical-guides/sentinel-3-olci/level-2/imt-neural-net)

[31] Ioannou I, Foster R, Gilerson A, Gross B, Moshary F, Ahmed S. Neural network approach for the derivation of chlorophyll concentration from ocean color. In: Hou WW, Arnone RA, eds. 2013/06. p. 87240P-P.

[32] Doerffer R. Algorithm theoretical bases document (ATBD) for L2 processing of MERIS data of case 2 waters, 4th reprocessing; 2015.

[33] Tilstone G, Mallor-hoya S, Gohin F, Couto AB, Sá C, Goela P, et al. Remote sensing of environment which ocean colour

algorithm for MERIS in north west European waters? Remote Sens Environ. 2017;189:132–51.

[34] Toming K, Kutser T, Uiboupin R, Arikas A, Vahter K, Paavel B. Mapping water quality parameters with Sentinel-3 ocean and land colour instrument imagery in the Baltic Sea. Remote Sens. 2017;9:1070.

[35] Santos Dos ACA, Calijuri MC, Moraes EM, Adorno MAT, Falco PB, Carvalho DP, et al. Comparison of three methods for chlorophyll determination: spectrophotometry and fluorimetry in samples containing pigment mixtures and spectrophotometry in samples with separate pigments through high performance liquid chromatography. Acta Limnol Bras. 2003;15:7–18.